

# MR Motion Correction of 3D Affine Deformations

G. Shechter<sup>1</sup>, E. R. McVeigh<sup>2</sup>

<sup>1</sup>Department of Biomedical Engineering, Johns Hopkins School of Medicine, Baltimore, MD, United States, <sup>2</sup>Lab of Cardiac Energetics, NHLBI, National Institutes of Health, DHHS, Bethesda, MD, United States

## Synopsis

MR motion correction is used to improve image quality while reducing total scan time. The Fourier nature of MRI is used to describe a technique for compensating for 3D affine transformations (translation + rotation + dilation + shear) of an object during the imaging process. We present the mathematical basis for this correction strategy and results of a simulated MR acquisition.

## Introduction

Motion during MRI causes blurring and ghosting artifacts [1]. Motion correction for translation [2], dilation [3], and rigid body [4] motion has been described. However, physiologic motion of soft tissue is more complex. We describe a motion correction technique for compensation of 3D affine deformations of the imaged volume. Affine deformations can describe translation, rotation, dilation (compression), and shear in 3 orthogonal directions. Manke [5] alluded to the ability to correct for affine transformations during an MR acquisition, but a detailed scheme has not yet been described.

## Methods

The class of 3D affine transformations  $\{A: \mathbb{R}^3 \rightarrow \mathbb{R}^3\}$  describes a global space warping with 12 degrees of freedom, which can be decomposed into 3D translations, rotations, scalings and shears. Equation 1 represents the 3D affine transformation of a point  $\mathbf{q} = \{q_x, q_y, q_z\}$  in homogeneous coordinates where  $R(\theta, \phi, \psi)$  is a 3x3 rotation matrix,  $(t_x, t_y, t_z)$  is a 3D translation vector,  $\{S_x, S_y, S_z\}$  are 3D scale factors, and  $\{S_{xy}, S_{xz}, S_{yz}\}$  are 3D shear parameters. Using properties of the Fourier transform, a relationship can be defined between  $F$ , the k-space representation of an imaged volume, and  $F'$ , the k-space of a 3D affine transformation of the imaged volume. The k-space point  $\mathbf{k} = \{k_x, k_y, k_z\} \in F$  maps to the point  $\mathbf{k}' = \{k'_x, k'_y, k'_z\} \in F'$  according to equations 2 and 3.

These equations can be used to motion correct an MR acquisition, by relating k-space samples of a deformed object to samples of the undeformed, or reference, configuration of that object. Consider an MR spin-warp 3D Fourier image acquisition. For prospective motion correction, before acquiring each line of k-space, an estimate of the amount of motion would be generated. Equations 2 and 3 would be used to modify the gradients in order to traverse a modified k-space trajectory in the Fourier space of the deformed imaging volume. This data would then be stored in the data matrix along the initial, undistorted, trajectory.

A 3D spin warp acquisition was simulated on a binary algebraic 3D heart phantom in a volume of  $64^3$  voxels. The volume was deformed by a 3D affine transformation whose magnitude varied sinusoidally. The motion was periodic with frequency  $f$ , so that at time  $t$ , the transformation parameters were calculated using the equation  $p = \bar{p} \sin(2\pi ft)$ , where  $\bar{p}$  represents any of the shear, rotation, or translation parameters. For dilation, the transformation parameters were calculated using the equation  $q = 1 + \bar{q} \sin(2\pi ft)$ . The image acquisition was simulated without and with the proposed prospective 3D affine motion correction.

## Results

Results of the simulated 3D MR spin warp acquisition are shown in Figure 1. The 3D affine motion model used for the simulation was defined by the parameters  $\bar{\theta} = -0.25$  rad,  $\bar{\psi} = 0.1$  rad,  $\bar{t}_x = \bar{t}_y = 2$  voxels,  $\bar{t}_z = -8$  voxels,  $\bar{S}_x = -0.2$ ,  $\bar{S}_z = 0.13$ ,  $\bar{S}_{xy} = 0.3$ ,  $\bar{S}_{xz} = -0.15$ , and  $\bar{\phi} = \bar{S}_y = \bar{S}_{yz} = 0$ . The TR was  $0.05f$ , and it was assumed that the TE was very short, so that there was no motion during the echo readout. Images obtained without motion correction show severe artifacts (column C). Correcting for previously described deformation modes (translation, scaling, and rotation) improves the images, but ghosting is still observed (column D). Prospective motion correction for the complete 3D affine case, which includes correction for shear, is shown in column E.

## Discussion

This work presents a method for MR motion correction of 3D affine deformations. Prospective correction of a known 3D affine deformation was validated by simulation. The prospective method maintains a regular and uniform sampling density in k-space, but would require gradient waveforms to be changed in real time on an MR scanner. Alternatively, a retrospective strategy can be implemented without changing the data acquisition procedure. Each k-space line would be acquired along with a measure of the deformation at that moment. Later, each k-space line would be moved to a new position in the Fourier volume according to Equations 2 and 3, which might result in a non-uniform sampling density. A regridding algorithm would be needed to regularize the k-space data. Further work is required to develop methods for measuring and modeling affine deformation of tissues and organs in vivo.

## Acknowledgements

J. Andrew Derbyshire, Luis F. Gutiérrez, Peter Kellman

## References

- [1] Wood ML et al, Med Phys 1985; 12:143-15
- [2] Korin HW et al, Magn Reson Med 1989; 12:99-113
- [3] Haacke EM et al, Magn Reson Imaging, 1986; 4:359-376.
- [4] Derbyshire JA et al, J Magn Reson Imaging 1998; 8:924-932
- [5] Manke D et al, J Magn Reson Imaging 2002; 15:661-671

## Equations

$$1. \begin{bmatrix} q'_x \\ q'_y \\ q'_z \\ 1 \end{bmatrix} = \begin{bmatrix} R(\theta, \phi, \psi) & t_x \\ & t_y \\ & t_z \\ 0 & 0 & 0 & 1 \end{bmatrix} \begin{bmatrix} 1 & S_{xy} & S_{xz} & 0 \\ 0 & 1 & S_{yz} & 0 \\ 0 & 0 & 1 & 0 \\ 0 & 0 & 0 & 1 \end{bmatrix} \begin{bmatrix} S_x & 0 & 0 & 0 \\ 0 & S_y & 0 & 0 \\ 0 & 0 & S_z & 0 \\ 0 & 0 & 0 & 1 \end{bmatrix} \begin{bmatrix} q_x \\ q_y \\ q_z \\ 1 \end{bmatrix}$$

$$2. F(k_x, k_y, k_z) = (S_x S_y S_z)^{-1} e^{i(k'_x t_x + k'_y t_y + k'_z t_z)} F'(k'_x, k'_y, k'_z)$$

$$3. \begin{bmatrix} k'_x \\ k'_y \\ k'_z \end{bmatrix} = R(\theta, \phi, \psi) \begin{bmatrix} 1 & 0 & 0 \\ -S_{xy} & 1 & 0 \\ (S_{xy} S_{yz} - S_{xz}) & -S_{yz} & 1 \end{bmatrix} \begin{bmatrix} S_x^{-1} & 0 & 0 \\ 0 & S_y^{-1} & 0 \\ 0 & 0 & S_z^{-1} \end{bmatrix} \begin{bmatrix} k_x \\ k_y \\ k_z \end{bmatrix}$$

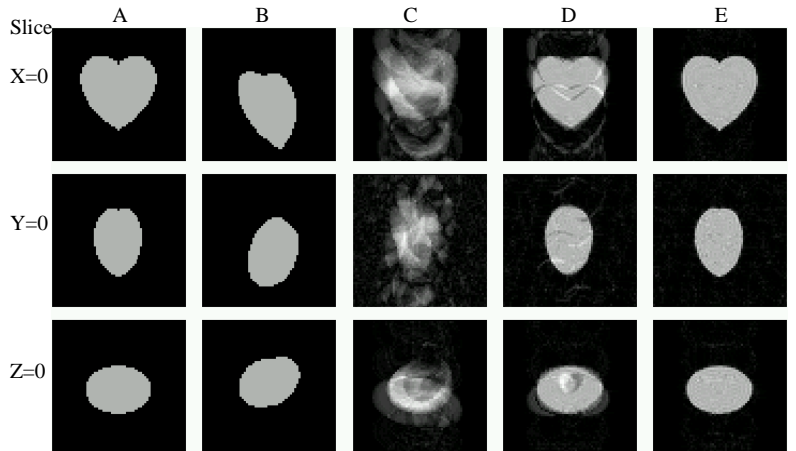


**Figure 1.** Three orthogonal imaging slices. (A) The static heart phantom. (B) The phantom at its maximum 3D affine deformation. (C) Simulated images obtained with a 3D spin-warp imaging technique, while the phantom is undergoing a periodic 3D affine deformation with a sinusoidally varying magnitude. (D) Similar to (c), but motion correction for translation, rotation, and scaling is used. Ghosting due to the uncorrected shear deformation is observable. (E) Full 3D affine motion correction applied prospectively to the 3D spin warp acquisition.